

# Modelling granite migration by mesoscale pervasive flow

A.M. Leitch<sup>a,\*</sup>, R.F. Weinberg<sup>b,1</sup>

<sup>a</sup> Department of Earth Sciences, Memorial University of Newfoundland, St John's, NF, Canada A1B 3X5

<sup>b</sup> Institute of Earth Sciences, Uppsala University, Uppsala, S-752 36 Sweden

Received 30 July 2001; received in revised form 6 March 2002; accepted 11 March 2002

## Abstract

Mesoscale pervasive magma migration leads to granite injection complexes, common in hot crustal terranes. Pervasive migration is limited by magma freezing when intruding cold country rock. Here, we explore numerically the feedback mechanism between magma intrusion and heating of the country rock, which allows younger intrusive batches to reach increasingly shallower/cooler levels. This process relies on the higher solidus temperature of a rock compared to that of its melt, once melt is segregated. We define the 'free-ride layer' as the region above the melt source, where magma may freely migrate because rock temperature is above melt solidus. The top of the free-ride layer, which corresponds to the melt solidus ( $T_S$ ) isotherm, is at the 'limiting depth',  $z_S$ . After magma passes through the free-ride layer, the magma 'front' is always at the limiting depth. We modeled the thickening and heating of the crust above the source as melt at its liquidus ( $T_L$ ) intrudes it pervasively from below. We found that: (a) magma quickly warms crust below  $z_S$  to about  $T_L$ , forming a step in temperature at  $z_S$ ; (b) the front ( $z_S$ ) moves up through the crust as more magma is intruded; (c) as magma is emplaced at the front, a mingled layer of about half magma half crust forms below it, so that the total rise of the front corresponds approximately to half of the thickness of magma added to the free-ride layer; (d) the rate of rise of the front depends on the temperature difference between crust and  $T_L$ , and slows down as the magma front rises; (e) for most reasonable intrusion rates and volumes, the crust above  $z_S$  feels little influence of the intrusion, because the diffusion time scale is much smaller than the rise rate of the front. In summary, pervasive migration is an efficient way of heating the lower to middle crust, and can result in an injection complex several kilometers thick, consisting of about half magma and half original crust. © 2002 Elsevier Science B.V. All rights reserved.

**Keywords:** granites; anatexis; migration; injection; intrusions

## 1. Introduction

Pervasive migration, where magma moves upwards through an extensive network of channels, is an alternative method for crustal magma migration to dyking and diapirism. Granite magma injection complexes are thought to result from magma migrating pervasively through an interconnected network of blobs and sheets, of scales varying between millimeters and tens of meters

\* Corresponding author. Tel.: +1-709-737-3306;

Fax: +1-709-737-2589.

E-mail address: aleitch@mum.ca (A.M. Leitch).

<sup>1</sup> Present address: Centre for Global Metallogeny, University of Western Australia, Crawley WA 6009, Australia.

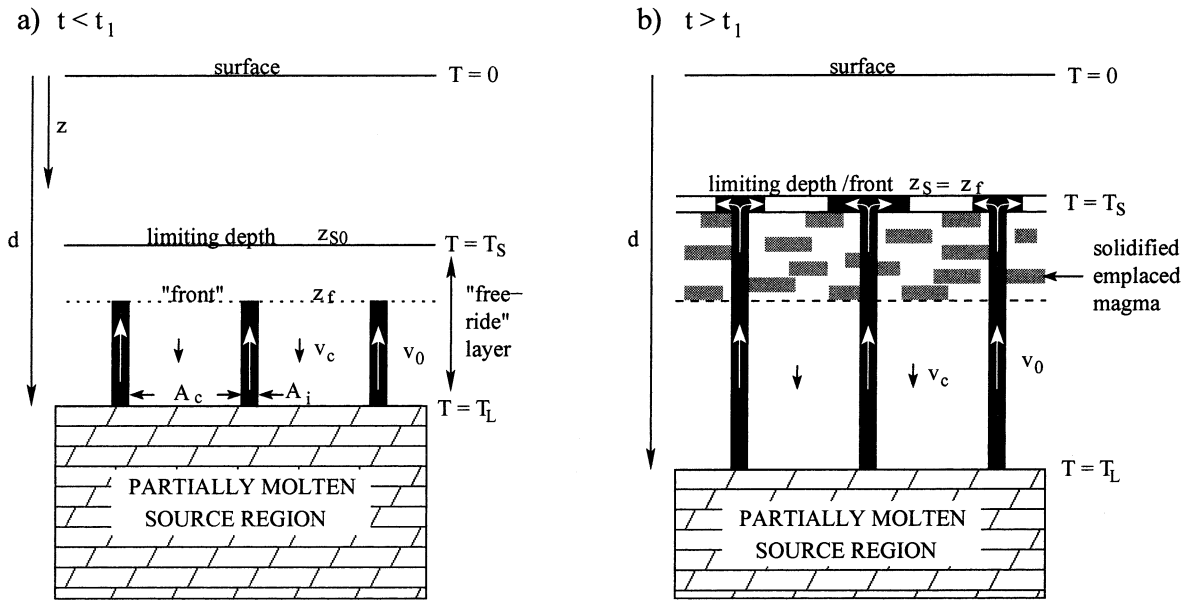


Fig. 1. Sketch of conceptual model of pervasive intrusion developed here.

[1–4]. Sawyer et al. [5] argued, based on a combination of textural and structural observations, that melt may be present in migmatites for a protracted period of time, during which tectonic stresses ‘cause melt to migrate from site to site in response to transient changes in pressure gradients resulting from the anisotropic nature of the rocks’. At least four mechanisms control pervasive magma migration [4]: (a) tectonic pumping [4,6]; (b) pervasive flow through hot, low-viscosity country rocks (where dyking is inhibited [7]); (c) volatile-driven intrusion, where magma follows volatile-rich phases [8]; and (d) local dyking.

When magma intrudes country rocks which are colder than the magma solidus, it will tend to freeze and stall at the contacts. Magma propagation through cold country rocks therefore requires a focused mechanism, such as dyking or diapirism, in which a central volume of magma can rise before it loses its heat. Because pervasive migration has neither the protective large volume of diapirs, nor the high flow speed of magmas in dykes, it requires country rock temperatures above the magma solidus. Weinberg and Searle [7] argued that the early pervasive migration history may control the mechanism of focused mi-

gration that follows. If pervasive migration gives rise to a well-connected network of magma channels, dyking may follow. Conversely, if it leads to the growth of a large buoyant body, diapirism may follow. Although the high-temperature requirement may seem very restrictive for pervasive migration, we envisage a feedback mechanism whereby heat advected with early magma batches will warm the crust, allowing later batches to reach shallower levels.

The key factor for the viability of pervasive migration is that the solidus temperature of a rock is commonly higher than the solidus temperature of the partial melt it produces, once melt is extracted from rock pores. For example, an amphibolite may start melting at 850–900°C but the granite melt it produces may have a solidus temperature at 650–750°C. This temperature difference between solidi,  $\Delta T_{LS}$ , allows melt to intrude a layer above the source which, though solid, is at temperatures above the melt solidus. We called this layer the ‘free-ride layer’, because melt will rise through it without freezing (Fig. 1). The initial width of this layer  $\delta z_1$  is  $\Delta T_{LS}$  divided by the average geothermal gradient:  $\delta z_1$  may be a few hundred meters or several kilometers depending

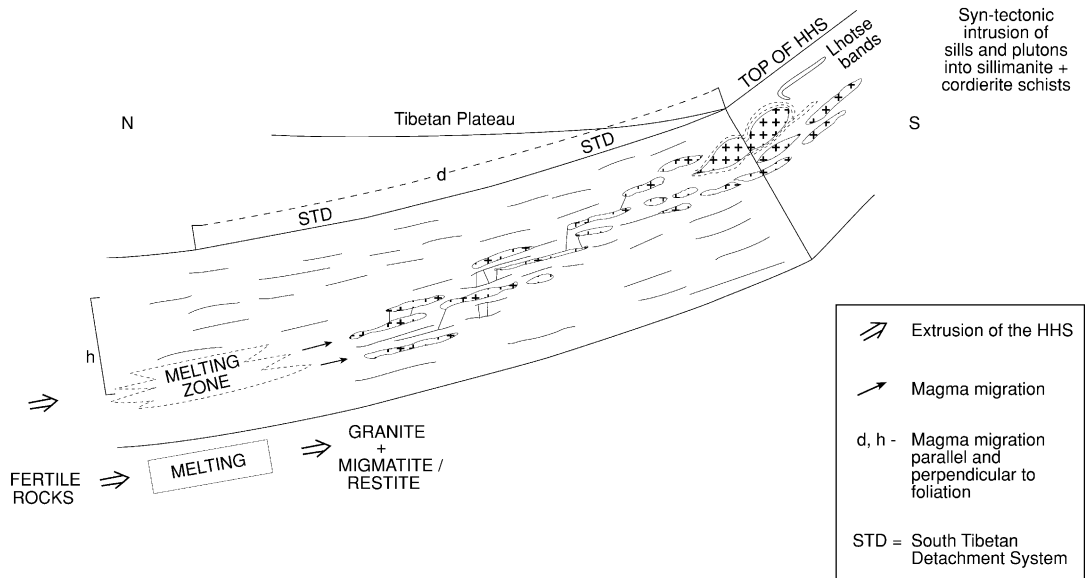


Fig. 2. Proposed crustal cross-section showing the formation of Himalayan leucogranites [8]. In this model the source zone is continuously renewed by slab extrusion. Young melts will tend to follow previously opened magma pathways until the pathway becomes too far from the source and a new pathway is opened. Width of figure corresponds to roughly 20 km.

on the geothermal gradient above the source. The temperature at the top of the free-ride layer equals the magma solidus temperature, and is the initial ‘limiting depth’ of pervasive migration. As the process develops, the limiting depth gradually migrates upwards, pushed by heat released by magma intrusion (Fig. 1), and a thickening injection complex or a pluton may develop.

Pervasive migration may occur in any crustal or mantle setting as long as the melt released from the source segregates into pockets sufficiently large as to be partially isolated from the solids (i.e. melt pockets larger than a couple of centimeters). In the continents we envisage two particularly favorable environments: underplated basalt melting crustal rocks, and crustal melting in collisional orogens. The dynamic environment of continental collisions may give rise to complex migration systems. In the Himalayas, melting during collision gave rise to the leucogranite masses which now intrude the High Himalayan Slab (HHS), the rock wedge being extruded between the South Tibetan Detachment System (STD) above and the Main Central Thrust (MCT) below (fig. 1 of [8]). In the High Himalayas of Khumbu, Nepal, there are voluminous leucogranitic injection

complexes overlain by large leucogranite plutons (commonly over a kilometer thick and several kilometers wide) emplaced below the South Tibetan Detachment (Fig. 2). Weinberg and Searle [8] envisaged that the melt source lay to the north (under the Tibetan Plateau) and that melt migrated mainly parallel to the north dipping regional foliation, but also locally across it, reaching increasingly higher stratigraphic levels as it travelled south. A steady-state situation may have developed where extrusion of the HHS brought fertile rocks into the melting zone so that melt could be continuously produced. Melt migration created a warm pathway across the wedge, linking the melting zone to the large leucogranite plutons cropping out to the south, in the High Himalayas. The magma frozen in the pathway makes up the injection complex below the leucogranite plutons (Fig. 2).

In this paper we explore the effects of pervasive melt migration using a simple, one-dimensional model of heat and mass transfer. We have identified key parameters which control the efficiency of pervasive magma migration in heating the free-ride layer and pushing the limiting depth to shallower crust.

Table 1  
Notation

Symbol	Meaning	Value
$A$	horizontal cross-sectional area or channel width	
$c_p$	specific heat	1500 J/kg/°C
$d$	layer depth	$d_0 = 36$ km
$g$	acceleration due to gravity	9.8 m/s <sup>2</sup>
$h$	height of computational cell	1/300
$L$	latent heat of intruding magma	$3 \times 10^5$ J/kg
$t$	time	
$t_1$	time to cross free-ride zone	
$t_2$	time to form step profile in $T$	
$t_3$	time for front to reach surface	
$T$	temperature	
$T_L$	liquidus of intruding magma	800–950°C
$T_S$	solidus of intruding magma	700–800°C
$v_0$	velocity of magma in channels	$2.5 \times 10^{-8}$ m/s
$V$	volume of crust or input	
$x$	volume fraction of input material	
$z$	depth, measured from the surface	
$z_S$	depth of the isotherm $T = T_S$	
$z_{S0}$	initial depth of isotherm $T = T_S$	
$z_2$	front depth at $t = t_2$	
$\kappa$	thermal diffusivity ( $k/\rho c_p$ )	$9 \times 10^{-7}$ m <sup>2</sup> /s
$\chi$	melt fraction within the magma	
Subscripts		
c	crust	
f	magma front	
fin	end of numerical run	
i	intruding magma	
0	initial condition ( $t = 0$ )	
L	liquidus	
S	solidus	
Dimensionless parameters		
Pe	Peclet number	250–4000
St	Stefan number	0–2
$\phi$	volume fraction of input channels	0.01–0.1
$\theta$	relative crustal temperature	0–1
$T'_S$	normalized solidus temperature	0.833, 0.875

## 2. A simple heat balance

We can judge whether pervasive input has the capability of heating the crust significantly with a simple heat balance calculation. All variables are defined in Table 1. If a layer of crust, volume  $V_c$  and temperature  $T_c$ , is intruded by magma of volume  $V_i$ , temperature excess  $\delta T_i = T_i - T_c$  and latent heat  $L$ , when the two volumes come to a

common temperature the temperature rise of the crust will be:

$$\Delta T_c = \frac{(L + c_p \delta T_i) V_i}{c_p (V_i + V_c)} = \frac{\text{excess heat of input}}{\text{total heat capacity}} \quad (1)$$

We assume the densities and specific heats  $c_p$  are the same. For  $L = 3 \times 10^5$  J/kg and  $c_p = 1500$  J/kg/K,

$$\Delta T_c = (200 + \delta T_i) \frac{V_i}{V_i + V_c} \quad (2)$$

In Table 2 we see that if new input makes up a significant fraction of the crust, the rise in temperature can be considerable.

## 3. Conceptual model and assumptions

A sketch of our conceptual model is given in Fig. 1. A crustal layer of initial thickness  $d_0$  overlies a partially molten source region from which magma rises through channels of cross-sectional area  $A_i$ , separated by crust of area  $A_c$ . The magma rises at vertical ‘seepage’ velocity  $-v_0$  relative to the surface, warming the adjacent crust and causing it to sink at velocity  $V_c$ . The upper limit of magma intrusion, at depth  $z_f$ , is called the magma ‘front’. The front propagates at speed  $-v_f = -v_0$  through the free-ride layer between the top of the source region and the limiting depth,  $z_{S0}$  (Fig. 1a).

At time  $t = t_1$ , the magma front reaches the limiting depth, and there the magma is emplaced, mingled with original crustal material (Fig. 1b). The fraction of magma at a given depth is denoted by  $x$ . When it is first emplaced the mingled material is at the magma solidus temperature  $T_S$ . For  $t > t_1$ , the limiting depth and the front depth are the same,  $z_S = z_f$ , and the front rises at a reduced velocity,  $v_f < v_0$ , because magma is diverted sideways as it is emplaced. With time  $z_S$  shallows and a sub-layer of mingled material builds up beneath it (Fig. 1b). New batches of magma warm the mingled material so after emplacement mingled material is always hotter than  $T_S$ .

Our conceptual model is two-dimensional but

the mathematical model is only one-dimensional. Each depth  $z$  is characterized by a unique temperature, a fraction  $x$  of injected material, a channel vertical velocity,  $-v_0$  or zero, and a ‘porosity’  $\phi = A_i/A$ , where  $A = A_i + A_c$ . We do not model the channel geometry or size (except relative to adjacent crust), and the heat transfer between channels and crust is assumed to be immediate. In summary, our assumptions are:

1. The model is one-dimensional: as material is injected into the layer from below, the bottom of the layer moves downward to conserve volume.
2. Magma enters the layer at its liquidus temperature  $T_L$ , which is also the crustal temperature at the bottom of the layer.
3. At any given depth and all times, the crust and magma are in thermal equilibrium.
4. Channel velocity  $v_0$  and ‘porosity’  $\phi$  are constant.
5. As magma is cooled below  $T_L$ , it releases latent heat but all crystals are carried upward until the entire unfractionated material is emplaced when it reaches the solidus temperature  $T_S$ .
6. Latent heat is released evenly through the interval  $T_L$  to  $T_S$ .
7. Once emplaced, the material is not remelted or remobilized, even if the temperature reaches  $T_L$ .
8. The original crustal material does not melt.
9. The physical properties of the crust and injected magma (density, thermal conductivity, specific heat) are the same.

All assumptions are made to simplify the problem so that it is mathematically tractable, and to enable us to gain insight into the first-order effects.

Assumption 1 implies no lateral spreading of

the crust, and that the source and injection complex have the same lateral dimensions. Beyond a certain point, as the layer of warm, weak crust builds up, this becomes unrealistic. The validity of assumption 3 is discussed in detail in Appendix A (**Background Data Set**<sup>2</sup>).

Assumptions 4 and 5 together say that magma is able to percolate upward at a constant rate until it solidifies. The velocity at which it rises results from a complex interaction between magma buoyancy, the mechanical properties of the crust, and external applied stress. The system is so complex that it is not possible at present to calculate magma velocity, which is therefore treated here as a variable. Regardless of the rate at which it rises, the ultimate height to which the magma can rise is determined by its solidification temperature (assumption 5).

Assumption 5 may seem particularly unrealistic, however relaxing it introduces significant mathematical complications, and it is not obvious how it should be relaxed. The rates at which crystals are dropped out of the magma and magma fractionates are unknown, and are likely to depend on the detailed mechanism of upward flow. The critical melt fraction (CMF) at which a given magma becomes effectively solid is somewhere between 30 and 50%. The exact value depends on wetting angles between melt and crystals, crystal size and shape distributions [9] and preferred crystal orientation. However, because the final 20–40% crystallization in a magma occurs very close to the solidus temperature [10] the magma will indeed become effectively solid close to the solidus and assumption 5 is not unreasonable. On the other hand, if a significant fraction of the magma crystallizes very close to the solidus temperature, then the latent heat is not released linearly, contrary to our assumption 6. However, as discussed in Section 5, after pervasive migration has continued for an initial period, the solidus–liquidus temperature difference occurs over a small depth interval so exactly where and at what temperature the crystals are dropped will not matter very much.

Table 2  
Temperature increase of the crust from Eq. 2

$V_i/(V_i+V_c)$	$\delta T_i$	$\Delta T_c$
0.10	0	20
0.25	0	50
0.50	0	100
0.50	100	150
0.60	150	210

<sup>2</sup> <http://www.elsevier.com/locate/epsl>

A justification for assumption 7 is that upon solidification the magma loses volatiles and will be harder to remelt. Assumption 8 is equivalent to assuming that the solidus of the layer is above the liquidus of the input magma (see Section 1).

#### 4. Equations and computer code

The governing equations for the one-dimensional heat and mass transfer problem outlined above are given here, in Sections 4.1 and 4.2. There are some similarities with pervasive flow of volatiles [11], but in that situation latent heat and crustal growth are unimportant. In Section 4.3 the meaning of the equations and the controlling parameters is discussed, and Section 4.4 is a brief description of the computer code.

##### 4.1. Derivation of equations

###### 4.1.1. Initial and boundary conditions

These are:

$$T(z) = T_L z \quad (0 \leq z \leq d_0, t = 0) \quad (3)$$

$$v_i = -v_0 \quad (z > z_f, t \geq 0) \quad (4)$$

$$v_c A_c + v_i A_i = 0 \quad (5)$$

$$T = \begin{cases} 0 & \text{at } z = 0 \\ T_L & \text{at } z = d \end{cases}$$

$$v_i = \begin{cases} 0 & \text{at } z = 0 \\ -v_0 & \text{at } z = d \end{cases}$$

$$d = d_0 + \frac{A_i}{A_c} v_0 t \quad (6)$$

That is, we start with a crustal layer thickness  $d_0$  with a linear profile of temperature  $T$  with depth (Eq. 3). Depth  $z$  and velocity  $v$  are measured downward from the surface. The velocity of magma in the channels  $v_i$  is constant everywhere below the magma front  $z_f$  (Eq. 4). In order to conserve mass, the upward flux of magma is

balanced by downward movement of the original crust (Eq. 5). Conditions at the surface and the base of the layer are given in Eq. 6. We note that as magma is injected, layer thickness  $d$  increases according to  $d = d_0 + v_c t$ .

###### 4.1.2. Equations for temperature

The general heat equation for a material which can change phase (such as a crystallizing magma) is, in one dimension [12]:

$$\frac{\partial T}{\partial t} = \kappa \frac{\partial^2 T}{\partial z^2} - v \frac{\partial T}{\partial z} - \frac{L(\chi, z)}{c_p} \left( \frac{\partial \chi}{\partial t} + \frac{\partial \chi}{\partial z} \right) \quad (7)$$

where  $\kappa$  is the thermal diffusivity and  $\chi$  is the melt fraction. The left-hand side of Eq. 7 is the change in temperature at a given depth  $z$  in the crust, and the terms on the right are diffusion, advection, and latent heat release respectively, at the same position.

In general,  $L$  is a function of  $\chi$  and  $z$ , and  $\chi$  can vary in a complex way with temperature, but for simplicity (see Section 3), we set  $L = \text{constant}$  and specify that  $\chi$  varies linearly between  $T_L$  and  $T_S$ :

$$\chi = \frac{T(z) - T_S}{\Delta T_{LS}} \quad (8)$$

where  $\Delta T_{LS} = T_L - T_S$ .

At a given depth below the magma ‘front’ (Fig. 1), we can write down separate heat equations for the ‘original crust’ (subscript c) and the injected magma (subscript i). The original crustal material does not melt (assumption 8 above) and so there is no latent heat term:

$$A_c \frac{\partial T}{\partial t} = c \kappa \frac{\partial^2 T}{\partial z^2} - A_c v_c \frac{\partial T}{\partial z} \quad (9)$$

For the injected magma (using Eq. 8):

$$A_i \frac{\partial T}{\partial t} = A_i \kappa \frac{\partial^2 T}{\partial z^2} - A_i v_i \frac{\partial T}{\partial z} - \frac{L A_i}{c_p \Delta T_{LS}} \left( \frac{\partial T}{\partial t} + v_i \frac{\partial T}{\partial z} \right) \quad (10)$$

Since we assume that the crust and input thermally equilibrate instantly (assumption 4),  $T$  is

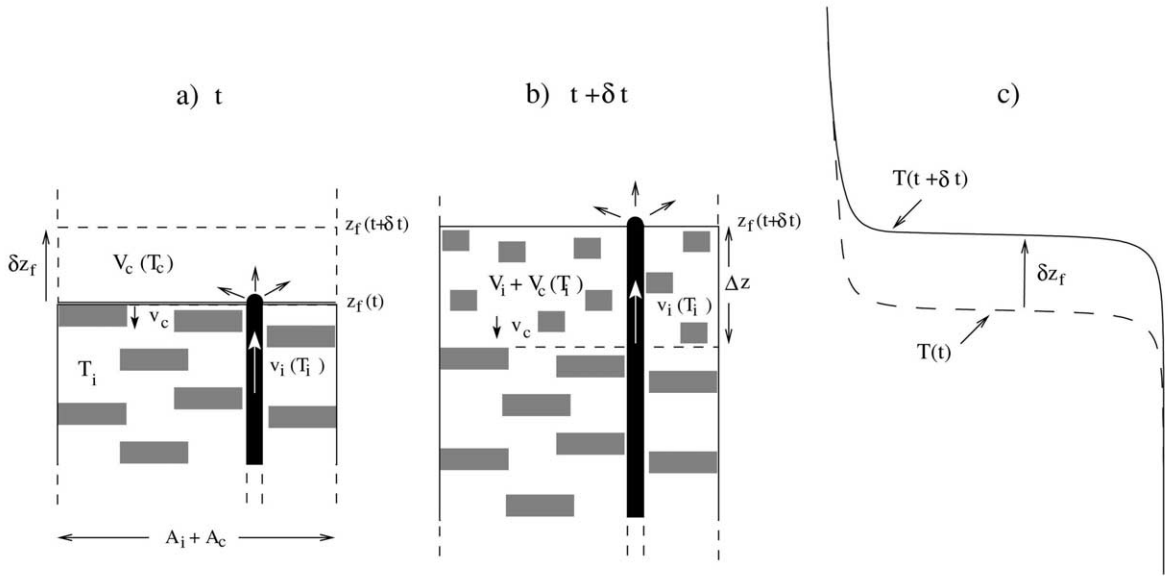


Fig. 3. Sketch of advancing front at times (a)  $t$  and (b)  $t + \delta t$ , and corresponding temperature profiles (c). Illustrates calculation of approximate front velocity  $v_f$  (Section 4.1.3).

the same in Eqs. 9 and 10. We add Eqs. 9 and 10, eliminate the second term on the right with the use of Eq. 5, and rearrange to find that for  $z > z_f$ :

$$\left(1 + \frac{L}{c_p \Delta T_{LS}} \frac{A_i}{A}\right) \frac{\partial T}{\partial t} = \kappa \frac{\partial^2 T}{\partial z^2} - \frac{v_i L}{c_p \Delta T_{LS}} \frac{A_i}{A} \frac{\partial T}{\partial z} \quad (11)$$

Above the front  $L=0$ , and Eq. 9 takes on the simple familiar form of thermal diffusion in one dimension:

$$\frac{\partial T}{\partial t} = \kappa \frac{\partial^2 T}{\partial z^2} \quad (z < z_f) \quad (12)$$

#### 4.1.3. $v_f$ and $x$

In addition to the boundary conditions and the heat equations Eqs. 11 and 12, to complete the problem, we need to know the front velocity  $v_f = dz_f/dt$  and how  $x$ , the volume fraction of the crust which is taken up by injected magma, varies with depth and time.

While the front is advancing through the free-

ride layer (Fig. 1a) we have:

$$v_f = v_i; \quad x = \frac{A_i}{A} \quad (z_f > z_{S0}) \quad (13)$$

The front reaches the limiting isotherm at time  $t_1$ :

$$t_1 = \frac{d_0 - z_{S0}}{v_0} \quad (14)$$

after which its advancement slows. In general for  $t < t_1$  we must find  $v_f$  numerically by balancing diffusion, advection and latent heat release at the front: however we can derive an approximate solution, valid after a certain time, if diffusion is relatively unimportant.

Without diffusion ( $\kappa \partial^2 T / \partial z^2 = 0$ ) a discontinuity in temperature would develop, since above the front the temperature would not evolve whereas below the front it would change due to advection. For most of our numerical runs advection dominates diffusion in the heat equation, and we find that a ‘step’ in the temperature profile develops (see Figs. 5–7) after a short time  $t_2$  (given for a linear initial geotherm by Eq. B3, Appendix B (Background Data Set)). After time  $t_2$ , we can

find an approximate analytical expression for  $v_f$  as follows.

We neglect diffusion and consider an interval of depth around the front (Fig. 3). The average temperature just above the front is  $T_c$ . Below the front,  $T$  varies from  $T_s$  to  $T_L$  over a certain depth interval. We assume the shape of the profile is steady with time so that the whole profile below the front rises at the same velocity  $v_f$  as the front itself.

In time interval  $\delta t$ , input magma of volume  $V_i$  mixes with crust of volume  $V_c$  and temperature  $T_c$ . Magma is emplaced at temperature  $T_s$ , releases its latent heat and is reheated. The front moves distance  $\delta z_f$  and the new mixed volume has thickness  $\Delta z$ . Magma in the channel (volume  $A_i \Delta z$ ) does not solidify. The net result is that some crust (volume  $V_c$ , temperature  $T_c$ ) has been heated to temperature  $T_L$ , and some magma (volume  $V_i - A_i \Delta z$ ) has released its latent heat. Conservation of heat gives:

$$c_p V_c (T_L - T_c) = L (V_i - A_i \Delta z) \quad (15)$$

Writing  $V_c$ ,  $V_i$  and  $\Delta z$  in terms of the  $\delta z_f$ ,  $\delta t$  and  $v_i$ , and rearranging we find:

$$v_f \approx \frac{\delta z_f}{\delta t} = v_i \frac{(L/c_p)(A_i/A)}{T_L - \theta T_s + (L/c_p)(A_i/A)} \quad (16)$$

In Eq. 16 we introduce:

$$\theta = T_c/T_s \quad (17)$$

which is a measure of how close the crustal temperature is to the solidus.

The volume fraction of injected magma  $x$  is given by  $x = V_i/(V_i + V_c)$ . Further algebra shows that  $x$  and  $v_f$  are related by:

$$x = \left[ 1 + \frac{v_f A_c}{v_i A_i} \right]^{-1}; \quad v_f = v_i \frac{A_i}{A_c} \left( 1 - \frac{1}{x} \right) \quad (18)$$

#### 4.2. Dimensionless equations

The equations can be non-dimensionalized using:

$$T' = \frac{T}{T_L}; \quad z' = \frac{z}{d_0}; \quad t' = t \frac{\kappa}{d_0^2}; \quad v' = v \frac{d_0}{\kappa} \quad (19)$$

where the primed variables are dimensionless. Defining the dimensionless variables:

$$\text{St} = \frac{L}{c_p \Delta T_{LS}}; \quad \phi = \frac{A_i}{A}; \quad \text{Pe} = \frac{v_0 d_0}{\kappa} \quad (20)$$

the initial and boundary conditions are:

$$T' = z' \quad (0 \leq z' \leq 1, \quad t' = 0) \quad (21)$$

$$v' = -\text{Pe} \quad (\text{for } z' > z'_f) \quad (22)$$

$$T' = \begin{cases} 0 & \text{at } z' = 0 \\ 1 & \text{at } z' = d' \end{cases}$$

$$v' = \begin{cases} 0 & \text{at } z' = 0 \\ -\text{Pe} & \text{at } z' = d' \end{cases}$$

$$d' = 1 + \left( \frac{\phi}{1-\phi} \right) \text{Pe} t' \quad (23)$$

and the heat equations (Eqs. 11 and 12) become:

$$(1 + \text{St} \phi) \frac{\partial T'}{\partial t'} = \frac{\partial^2 T'}{\partial z'^2} + (\text{St} \phi \text{Pe}) \frac{\partial T'}{\partial z'} \quad (z' > z'_f) \quad (24)$$

$$\frac{\partial T'}{\partial t'} = \frac{\partial^2 T'}{\partial z'^2} \quad (z' < z'_f) \quad (25)$$

Expressions for the front velocity of the front are:

$$v'_f = -\text{Pe}, \quad t' < t'_1 = (1 - z'_{s0})/\text{Pe} \quad (26a)$$

$$v'_f \approx -\text{Pe} \left[ 1 + \frac{(1 - \theta T'_s)/(1 - T'_s)}{\text{St} \theta} \right]^{-1}, \quad t' > t'_2 \quad (26b)$$

In the initial free-ride zone we have:

$$x = \phi, \quad z' > d' - (1 - z'_{s0})/(1 - \phi) \quad (27)$$

and at the front  $v'_f$  and  $x$  are related by:

$$x(z'_f) = \left[ 1 + \frac{v'_f}{\text{Pe}} \frac{1-\phi}{\phi} \right]^{-1}; \quad v'_f = \frac{\text{Pe}\phi}{1-\phi} \left[ 1 - \frac{1}{x} \right] \quad (28)$$

Substituting Eq. 26b into Eq. 28:

$$x(z'_f) \approx \left[ 1 + \frac{\text{St}(1-\phi)}{(1-\theta T'_s)/(1-T'_s) + \text{St}\phi} \right]^{-1} \quad (29)$$

### 4.3. Physical meaning of equations and parameters

Eq. 24 (cf. Eq. 11) says that temperature change at a given depth is due to diffusion of sensible heat (first term on right) and advection of latent heat (second term). Above the front (Eqs. 25 and 12) only diffusion can modify the temperature. (Here diffusion refers to conduction of heat up the geothermal gradient towards the surface.)

It is at first counter-intuitive that advection of latent heat alone modifies the temperature. Why does advection of sensible heat (i.e. the injection of hotter material from below) not change the temperature at a given depth? This result stems from the assumption of thermal equilibration between magma and crust, and from conservation of mass (Eq. 5). At any given depth, the upward advection of sensible heat  $A_i v_i \partial T / \partial z$  is exactly balanced by downward advection  $A_c v_c \partial T / \partial z$  as colder crust descends.

There are three dimensionless parameters controlling the system:  $\text{St}$ ,  $\phi$  and  $\text{Pe}$  (Eq. 20). The Stefan number  $\text{St}$  compares latent heat with heat capacity over the liquidus–solidus interval and so indicates how much of a temperature rise is associated with crystallization.  $\text{St}$ , together with the crustal temperature profile, determines  $x$  (Eq. 29). The ‘migration porosity’  $\phi$  is most significant in combination with the Peclet number  $\text{Pe}$ .  $\text{Pe}\phi/(1-\phi)$  is the volume flux of magma from the source, and so determines the growth rate of the layer.

$\text{Pe}$  is the ratio of the diffusion timescale  $\tau_k = d_0^2/\kappa$  and the advection timescale  $\tau_v = d_0/v_0$ . For many fluid flow situations,  $\text{Pe} \gg 1$  implies

that advection dominates diffusion in determining thermal evolution, however in this system we require  $\text{St}\phi\text{Pe} \gg 1$  instead (see Eq. 24). In our system  $\text{Pe}$  is a measure of how fast the magma moves,  $\text{St}\phi$  is a measure of how much heat it contains, and so  $\text{St}\phi\text{Pe}$  is a measure of how fast the heat moves.

### 4.4. Computer code

The fortran program PERVASE was written to solve Eqs. 24 and 25 with boundary conditions Eqs. 22 and 23. The crustal layer was divided up into cells of height  $h_0$  and finite difference equations were solved for each cell. Rather than using Eq. 26b for  $v_f$ , the full heat balance including the effects of diffusion was carried out in the cell containing the front. When the cell temperature exceeded  $T'_s$ , the front advanced to the next cell. Similarly,  $x$  was determined by how much input material was injected into each cell as the front advanced.

Problems where the volume of the domain changes with time always present a challenge in numerical work. Here, we allowed the individual cells to expand as new magma flowed into them, until they reached a critical height ( $1.6h_0$ ) when they were split into two. Thus, the number of cells increased with time and – because the cells beneath the magma front moved downward with time – the equations had a slightly different form to those above, which apply at fixed depths measured from the surface. Note that a cell only split while magma was being injected into it: because magma then continued to inject into only one of the parent cells, a high-frequency numerical ‘jitter’ was introduced into the profile for  $x$ . This jitter is smoothed by simple averaging in the curves below.

## 5. Results

The program PERVASE was run under the conditions listed in Table 3. In all cases, the initial thermal profile through the layer was linear, and the input conditions were constant. Figs. 4–7 show depth profiles of temperature  $T$  (thick

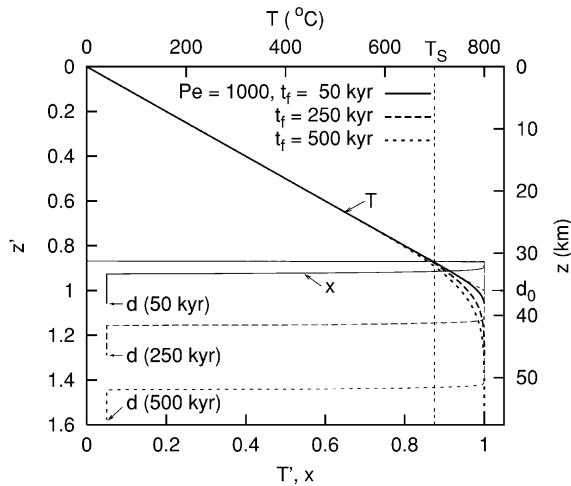


Fig. 4. Profiles of temperature  $T$  and emplaced fraction  $x$  at three times  $t$  after the start of pervasive intrusion. Run ST0, no latent heat (Table 3). Dimensional scales calculated assuming  $d_0 = 36$  km and  $T_L = 800^\circ\text{C}$ . Profiles for  $x$  have been smoothed (averaged over three to six points) to remove numerical ‘jitter’.

curves) and corresponding emplacement fraction  $x$  (thin curves) at various times  $t$ . Dimensionless scales are given on the left and bottom axes, and example dimensional scales are shown on the right and top axes. For converting to dimensional scales, we chose an initial layer depth  $d_0$  of 36 km and  $T_L$  of 800 or  $950^\circ\text{C}$ .

It is important to realize that the choice of  $d_0$  determines not only the dimensional depth scale on Figs. 4–7, but also the time scale for the curves of  $T$  and  $x$  (see Eq. 19). If we halved  $d_0$  to 18 km, then the times would be one quarter of those giv-

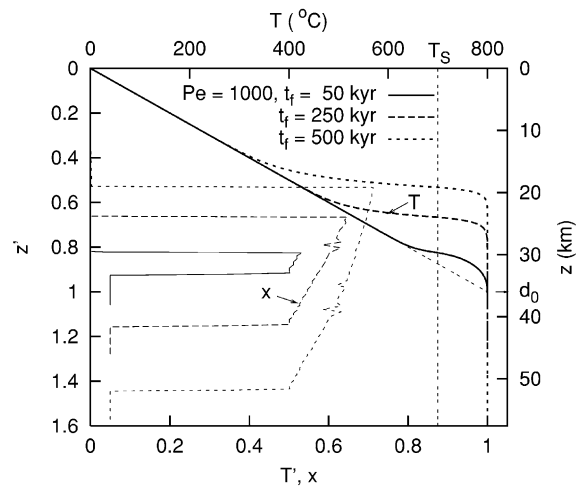


Fig. 5. Profiles of  $T$  and  $x$  for run ST2 with dimensionless latent heat  $St = 2$  (Table 3). Further details in caption for Fig. 4.

en. For example, in Fig. 5, the dashed curves would apply for  $t = 250/4 = 62.5$  kyr.

### 5.1. Choice of controlling parameters $St$ , $\phi$ , $Pe$

In our numerical runs we used the values of  $\kappa$ ,  $L$ ,  $c_p$ ,  $T_L$  and  $T_S$  given in Table 1, as representative of the crust. These values imply that  $St \approx 1.3$ – $2$ . Appropriate values for  $\phi$  and  $Pe$  are harder to choose. We picked  $\phi = 0.05$  as a reasonable ‘small’ number.  $Pe$  depends on both the initial layer depth  $d_0$  and the injection velocity  $v_0$ . As mentioned in Section 3, we have little handle on  $v_0$ . A lower limit might be a tectonic time scale of a

Table 3  
Conditions of numerical runs

Run	$St$	$\phi$	$Pe$	$St\phi Pe$	$T'_S$	$t'_{fin}$	$t_{fin}$ (kyr)	$t_1$ (kyr)	$t_2$ (kyr)
ST0	0	0.05	1000	0	0.875	0.011	500	5.7	$\infty$
ST2	2	0.05	1000	100	0.875	0.011	500	5.7	125
PHI1	0.67	0.10	1000	67	0.833	0.0033	150	7.6	243
PHI05	1.33	0.05	1000	67	0.833	0.0033	150	7.6	244
PHI01	1.33	0.01	5000	67	0.833	0.0033	150	1.5	232
PE250	2.0	0.05	250	25	0.875	0.0263	1,200	22.8	502
PE1000	2.0	0.05	1000	100	0.875	0.0066	300	5.7	125
PE4000	2.0	0.05	4000	400	0.875	0.0016	75	1.4	31
ZF	2.0	0.05	1000	100	0.875	0.042	2,500	5.7	125

Dimensional times  $t_{fin}$ ,  $t_1$ ,  $t_2$  calculated assuming  $d_0 = 36$  km and  $\kappa = 9 \times 10^{-7}$  m<sup>2</sup>/s.

few cm/yr ( $v_0 \approx 10^{-9}$  m/s,  $Pe \approx 40$ ), and an upper limit might be determined by buoyancy-driven flow rate in dykelets of cm to dm width (see Appendix A (Background Data Set)) ( $v_0 \approx 5 \times 10^{-6}$  m/s,  $Pe \approx 2 \times 10^5$ ). For most numerical runs, we chose an intermediate value of  $Pe \approx 1000$  which implies  $v_0 \approx 2.5 \times 10^{-8}$  m/s (80 cm/yr). The most important parameter for the thermal evolution of the crust, the product  $St\phi Pe$  (Section 4.3), was varied from 0 to 400.

### 5.2. Run ST0: no latent heat

For run ST0 the input magma had no latent heat. This case has no physical reality, however it is useful in emphasizing the role of latent heat in pervasive intrusion. Fig. 4 shows profiles of  $T$  and  $x$  at three times after the start. Principal features are:

1. Layer depth  $d$  increases steadily with time.
2. The depth  $z_S$  of the limiting isotherm  $T_S$  does not change, i.e. once it is through the free-ride zone, the front does not advance.
3. The temperature profile above  $z_S$  does not change.
4. There is a rounded ‘corner’ in the temperature profile at depth  $d_0$  ( $z' = 1$ ) where the initial linear gradient bends to become vertical.
5. In the lowermost part of the layer  $x = \phi$ . It then jumps to  $x = 1$ , and drops to zero above  $z_S$ .

These features can be understood from the governing equations. For  $St = 0$  ( $L = 0$ ) the heat equation below the front Eq. 24 reduces to the diffusion equation Eq. 25, according to which the temperature profile should not evolve at all due to advection. If diffusion was negligible, we would expect the original geotherm up to  $z' = 1$  to remain unchanged, and for it to be underlain by a growing layer at temperature  $T' = 1$ . There would be a sharp ‘corner’ at  $z' = 1$  where the temperature gradient changed. This is almost what is observed in Fig. 4, except that, under the run conditions of case ST0, diffusion is not negligible, and over time the ‘corner’ at  $z' = 1$  becomes rounder (point 4 above).

The lowermost portion of the layer where  $x = \phi$

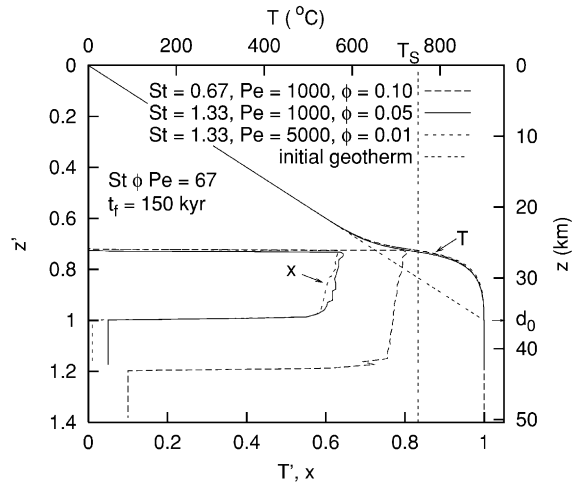


Fig. 6. Profiles of  $T$  and  $x$  for runs PHI1, PHI05 and PHI01, for which  $St\phi$  is the same, but relative area of channels  $\phi$  is 0.1, 0.05 and 0.01 respectively (Table 3). Dimensional scales calculated assuming  $d_0 = 36$  km and  $T_L = 900^\circ\text{C}$ .

is the original free-ride zone (Eq. 27). Here  $x$  is simply the fraction of crust taken up by the channels. Once through this zone, magma is emplaced where  $z = z_S$ . Continued emplacement at this unchanging depth results in a growing layer of unmixed ( $x = 1$ ) input material. The paradox that advection of hotter material from below does not modify the temperature profile is explained in Section 4.3.

### 5.3. Run ST2: including latent heat

Fig. 5 shows profiles of  $T$  and  $x$  for run ST2, which has  $St = 2$  (e.g.  $L = 3 \times 10^5$  J/kg released between  $T_L = 800^\circ\text{C}$  and  $T_S = 700^\circ\text{C}$ ). These profiles are very different from those in Fig. 4. We see:

1. The temperature profile has a stepped appearance around the  $T_S$  isotherm, with the original gradient at shallow depths and  $T \approx T_L$  at greater depths.
2. The limiting isotherm  $T_S$  shallows with time.
3. The corners of the step at  $T_S$  are rounded.
4. In the original free-ride zone  $x = \phi$ . Above this,  $x$  jumps to about 0.5, then increases slowly towards shallower depths until it drops to zero above  $z_S$ .

As Eq. 24 shows, for non-zero  $St$  the temperature profile below the front is modified by advection. To start with (curve for  $t = 50$  kyr), latent heat is deposited in the crust in the free-ride zone as the magma passes through, and the temperature of the crust rises. Once it reaches the top of the free-ride zone the magma is emplaced, and the remaining latent heat is used to heat the colder surrounding crust to  $T'_s$ . Thus the limiting isotherm rises.

As time goes on (curves for  $t = 250, 500$  kyr) the front advances and the crust underneath the front continues to warm. In a time  $t_2$  (125 kyr, Eq. B3, Appendix B (Background Data Set)) heat transfer from magma in the channels has raised the temperature below the front to about  $T_L$ , and for  $t > t_2$  the profile contains a step. From then on, all latent heat is deposited close to the front. The rounded corners of the step are due to diffusion.

The magma volume fraction  $x$  depends on how much latent heat is required to raise the crust just above the front to  $T_L$  (see Section 4.1.3), so it depends mainly on the temperature of the crust and the latent heat. The profiles of  $x$  in Fig. 5 reflect active emplacement at the front and the history of previous front injection below it: the bottom of the three profiles is identical, just shifted to greater depth as the injection complex thickens. The increase in  $x$  at shallower depths is due to the magma intruding into progressively colder country rock (see Section 5.6).

#### 5.4. Runs PH11, PH105, PH101: influence of $\phi$

The relative area of the injection channels in the crust,  $\phi$ , is most important when it is combined with other parameters. The volume flux of magma through the crust is  $Pe\phi$ , and the latent heat flux is  $St\phi Pe$ . For small  $St\phi$ , Eq. 24 shows that only the product  $St\phi Pe$  is important in thermal evolution. Fig. 6 displays  $T$  and  $x$  at the same time  $t_{fin}$  for runs PH11, PH105 and PH101, which all have  $St\phi Pe = 67$ .

PH11 and PH105 have different  $\phi$  but the same value of  $St\phi$  (see Table 3). The temperature profiles for these two cases are identical. However, the profiles of  $x$  and the layer thicknesses  $d$  are quite different. The total volume of magma in-

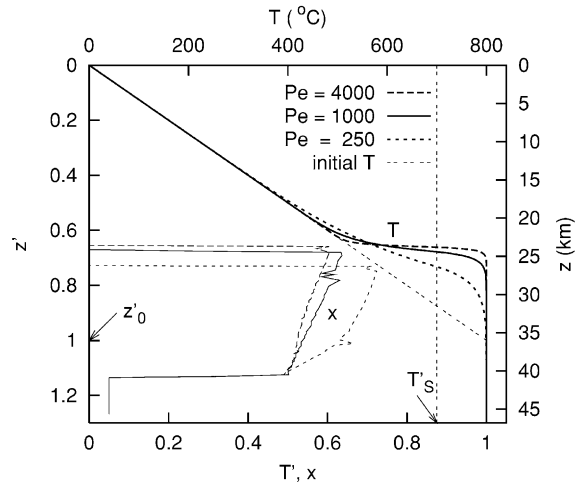


Fig. 7. Profiles of  $T$  and  $x$  for three values of  $Pe$  (and  $St\phi Pe$ ). Runs PE250, PE1000 and PE4000 (Table 3). Times  $t_f$  chosen such that each run has the same volume of injected magma.

truded past a given level in the crust is  $V'_{tot} = Pe\phi t'_{fin}$ . In case PH11 ( $\phi = 0.1$ ) the amount of intruded magma is twice as great as in case PH105 (although the intruded latent heat is the same) and therefore the increase in  $d$  and the integrated  $x$  are twice as great.

For runs PH101 and PH105 the product  $Pe\phi$  is the same, so the amount of intruded magma and the profiles of  $x$  are very similar. Because  $St\phi$  is small, the temperature profiles of the two runs are also very similar though not identical.

#### 5.5. Runs PE250–PE4000: influence of $St\phi Pe$

The relative importance of advection and diffusion on the crustal temperature profile is given by  $St\phi Pe$  (Section 4.3). As  $St\phi Pe$  increases ( $\gg 1$ ), advection dominates and the temperature profile develops a steepening ‘step’. This is illustrated in Fig. 7, which displays profiles for three values of  $St\phi Pe$ . In the figure,  $St$  and  $\phi$  are kept constant so that the profiles of  $x$  are comparable, and  $Pe$  is increased by increasing  $v_0$ . A faster  $v_0$  causes the system to evolve more quickly, so there is less time for diffusion to occur. The times  $t'_{fin}$  have been chosen such that the same amount of magma (and latent heat) has been added to the layer ( $St\phi Pe t'_{fin}$  constant). We see that the profiles are

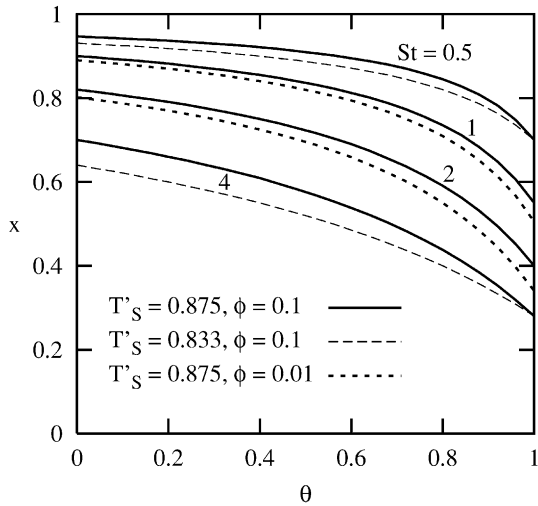


Fig. 8. Plots of  $x$  as a function of relative crustal temperature  $\theta = T_c/T_s$ , for various values of  $St$  (numbers next to curves), with  $\phi = 0.1$  and  $T'_S = 0.875$  (e.g.  $T_L = 800^\circ\text{C}$ ,  $T_s = 700^\circ\text{C}$ ). Dashed lines for  $St = 0.5$  and  $4$  illustrate the effect of changing  $T'_S$  to  $0.833$  (e.g.  $T_L = 900^\circ\text{C}$ ,  $T_s = 750^\circ\text{C}$ ). Dotted lines for  $St = 1$  and  $2$  show the effect of changing  $\phi$  from  $0.1$  to  $0.01$ .

broadly similar, but for smaller  $St\phi Pe$  – particularly for case PE250 – the step in the geotherm is rounder,  $x$  is higher and  $z'_s$  deeper.

### 5.6. $x$ and the front velocity, $v_f$

Once the step profile has formed ( $t > t_2$ ), an approximate expression for  $x$  as a function of the temperature just above the front is given by Eq. 29, where  $\theta$  (Eq. 17) is a measure of crustal temperature and varies from 1 (when the front first arrives at the limiting isotherm) to 0 (at the surface). Unbroken lines in Fig. 8 show plots of  $x$  versus  $\theta$  for a range of  $St$  at a given  $T'_S$  and  $\phi$ . The curves illustrate that  $x$  increases smoothly with crustal temperature, and that the emplaced magma is always a significant fraction of the mingled layer ( $> 30\%$ ). The dotted and dashed lines show that reasonable variations in  $T'_S$  and  $\phi$  do not change these basic features.

Eq. 29 applies in the limit of large  $Pe$  and for  $t > t_2$ . Analytical expressions for  $t_2$ ,  $z_f(t)$  and  $x(z, t)$  are derived for the special case of a linear geotherm in Appendix B (Background Data Set).

In dimensionless form they are:

$$t'_2 = 2 \frac{(1 + St\phi)}{PeSt\phi} (1 - z'_0) = 2 \frac{(1 + St\phi)}{St\phi} t'_1 \quad (30)$$

$$z'_f(t') = 1 - St\phi(1 - z'_0) \left[ \left( 1 + \frac{2Pe t'}{St\phi(1 - z'_0)} \right)^{\frac{1}{2}} - 1 \right] \quad (31)$$

$$x(z', t') = 1 - (1 - \phi) \left[ 1 + \frac{2(1 - \phi)(1 - z') + \phi Pe t'}{St(1 - z'_0)} \right]^{-\frac{1}{2}} \quad (32)$$

Eq. 30 equals Eq. B3 (Background Data Set); Eq. 31 equals Eq. B11 (Background Data Set); Eq. 32 equals Eq. B16 (Background Data Set).

The analytical and numerical results for  $T$  and  $x$  are compared in Fig. 9. The good agreement indicates that the values of  $Pe$  which we have been using are large enough that Eq. 29 is a reasonable approximation. Thus, as long as an injection complex is sufficiently deep, field observations of  $x$  together with good estimates of  $St$  and  $T'_S$  may give an indication of the temperature profile in the crust at the time of injection.

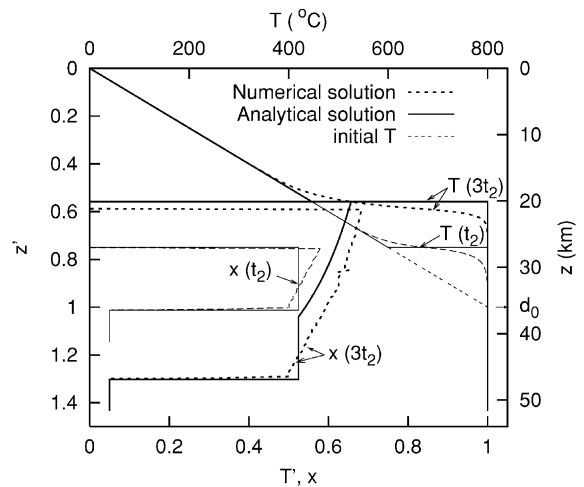


Fig. 9. Comparison of numerical and analytical results for profiles of  $T$  and  $x$  at times  $t = t_2$  and  $t = 3t_2$  where  $t_2$ , the time taken for a step to form, is given by Eq. 31 (run PE1000, Table 3). Dimensional scales assume  $T_L = 800^\circ\text{C}$ ,  $d_0 = 36 \text{ km}$ .

### 5.7. Run ZF: long time behavior

Fig. 10A and B shows how the depth of the magma front  $z'_f$  and the layer thickness  $d'$  vary with time for case ZF, which is the same as case PE1000 extended to longer times (2.5 Myr). The magma front rises quickly (at velocity  $v_0$ ) through the initial free-ride zone, reaching  $z'_{s0}$  at time  $t'_1$ . The front then rises at velocity  $v'_f$  (Eq. 26b), slowing as it encounters colder crust. If diffusion is neglected (analytical solution from Appendix B (Background Data Set)), the front reaches the surface in time  $t_3$  where

$$t'_3 = \frac{1}{\text{Pe}} \left[ 1 + \frac{1}{2\text{St}\phi(1-z'_{s0})} \right] \quad (33)$$

Eq. 33 equals Eq. B17 (Background Data Set).

When diffusion is included (numerical solution) the front stalls at shallow depth where all advected heat is conducted to the surface. In practice, it is unlikely that this stage is reached, because by then the layer has obtained unreasonable thickness. Thus, it is likely that pervasive migration is limited by the availability of magma and not by the effects of thermal conduction near the surface.

### 5.8. Summary

From Figs. 5–8, we see that pervasive migration modifies the original geothermal gradient by introducing a steep change in temperature at the position of the magma front (where  $x$  first becomes non-zero), and that this front advances to shallower depths with time. Below the magma front the temperature is approximately  $T_L$ . The sharpness of the step depends on  $\text{St}\phi\text{Pe}$ , and the rate of advancement of the front  $v_f$  depends also on the initial geotherm. The fraction  $x$  of injected magma in the injection complex depends mainly on  $\text{St}$  and relative crustal temperature  $\theta$ .

## 6 Discussion and conclusions

We have developed a simple mathematical and numerical model which captures some of the es-

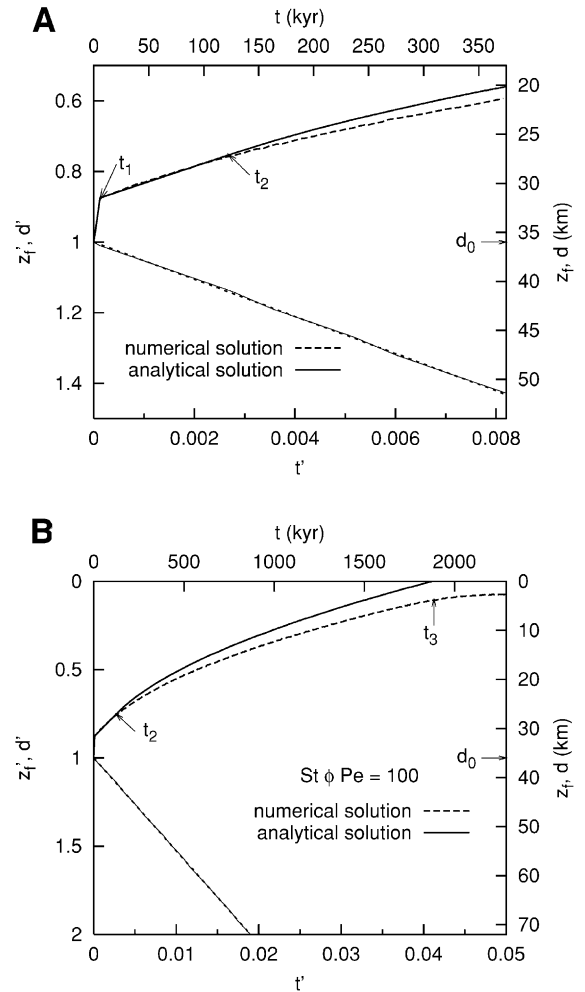


Fig. 10. The depth of the magma front  $z_f$  and the layer thickness  $d$  vs. time (A) for moderate time, (B) for long time. Run ZF (Table 3) and analytical results from Appendix B (Background Data Set). Analytical and numerical results give the same linear increase of  $d$  with time.

sential physical processes involved in pervasive magma migration. We have identified the key controlling parameters ( $\text{St}$ ,  $\text{Pe}$  and  $\phi$  – Section 4.3), and investigated how pervasive migration influences the temperature profile in the crust and the fraction  $x$  of crust taken up by the migrating magma.

The models show that during pervasive migration the layer of rock intruded by magma is gradually heated to temperatures approaching the magma liquidus, and magma is emplaced at the

depth of the melt solidus isotherm,  $z_s$ . This depth, corresponding to the magma ‘front’, shallows with time because of latent heat advected with the rising magma, resulting in a widening injection complex with approximately half crustal rock and half granite. The total vertical thickness of the complex is thus about twice the thickness of magma added to the crust. The rate at which the magma front moves upwards decreases as the front migrates to shallower levels, because the magma is being added to progressively colder crust. This implies that the process becomes inefficient in shallow crustal levels. How far the front rises depends, of course, on the geothermal gradient. Our models have all employed a simple linear gradient: if the gradient shallows with depth, as it generally does in the Earth’s crust, the front will rise closer to the surface than shown in our examples.

Interestingly, while the temperature below the migrating front approaches the magma liquidus, the temperature of the crust above the front remains largely unaffected (Figs. 5–7). This is because the time scale of pervasive migration in the models ( $\sim 10^4$ – $10^5$  a) is typically much shorter than that for diffusion ( $\sim 10^6$ – $10^7$  a). If pervasive migration occurs in pulses over a period of several million years, then there will be time for thermal relaxation and the overlying crust will be warmed, however, specially during an active pulse the temperature profile in the crust may be far from a steady-state geothermal gradient. Hot temperatures and partial melt at depth may be accompanied by average or even low heat flux at the surface.

Like the Khumbu area in Nepal described in Section 1, there are several examples worldwide of injection complexes. The Shuswap metamorphic core complex in the Canadian Cordillera, has 15 km of structural section exposed. It has anatectic migmatites at the base, representing magma source, structurally connected through a 5–10 km wide injection complex, to leucogranite laccoliths at the top [13,14]. The pervasive injection complex is composed of leucogranite and pegmatite pods and veins, intruding rocks with evidence for incipient partial melting. The laccolith is emplaced below a shallow-dipping fault

zone. Structural connection and similar leucogranite ages suggest that the exposures represent a frozen magma migration pathway from source to laccolith [14]. Similarly, the Pangong injection complex, NW Himalayas is thought to represent frozen pervasive flow of magma towards overlying plutons, possibly the large Karakoram Batholith cropping out in the vicinity [8]. In this area garnet-bearing leucogranites pervasively intruded amphibolites and migmatites. The high temperature of the country rocks at the time of intrusion is evidenced by similar zircon U–Pb ages of garnet leucogranites and in situ migmatite melt pods. As argued by Weinberg and Searle [8], high temperature of the country rock inhibited transport of leucogranite magma in dykes, but permitted pervasive intrusion of leucogranite and viscous flow of country rock.

These field relations show that partially molten zones may be overlain by injection migmatite zones several kilometers thick, capped by a thick region of melt accumulation. The scale, the interconnected nature and the similar volumes of host crust and injected leucogranites within the injection zones fit our simple model of pervasive migration. However, in the field we do not see evidence of an ‘original’ free-ride zone of smaller magma fraction between the source and the injection complex (Figs. 5–7), and our models do not predict the accumulation of magma in large bodies at the top of the complex.

Nature is not limited by our simplifying assumptions (Section 3), so we expect some deviations from the model predictions. In particular, as the front shallows and  $x$  increases, the melt may accumulate in pools rather than being distributed through the crust. The pools may then focus the emplacement of later melt, so that a sequence of large sills or a pluton is formed. The top of the surviving injection complexes may represent the maximum practical fraction of magma the crust can hold before the network breaks up into sills. Also, the proximity of the laccoliths at the top of the Shuswap complex with a fault zone suggests that a major rheological change within the crust along the magma path may cause the pervasive migration to stall and magma to accumulate. In nature, unlike our model, there is probably no

sharp distinction between the channels which carry the magma to the front and the injection complex of emplaced magma, thus we might not see the sharp change in  $x$  between the original free-ride zone and the injection complex seen in the models. This may be particularly true if the injection is pulsed and new pulses open up different channels.

### Acknowledgements

We thank Mike Brown, J.L. Vigneresse and an anonymous reviewer for their helpful comments. R.F.W. thanks Ed Sawyer and Olivier Vanderhaeghe for discussion on migmatites and pervasive migration processes. A.M.L. gratefully acknowledges financial assistance from the NSERC grants of Michael Rochester and Garry Quinlan. R.F.W. gratefully acknowledges a research fellowship from NFR. *[AC]*

### References

- [1] M. Brown, The generation, segregation, ascent and emplacement of granite magma: the migmatite-to-crustally derived granite connection in thickened orogens, *Earth Sci. Rev.* 36 (1994) 83–130.
- [2] W.J. Collins, E.W. Sawyer, Pervasive granitoid magma transfer through the lower-middle crust during non-coaxial compressional deformation, *J. Metam. Geol.* 14 (1996) 565–579.
- [3] M. Brown, G.S. Solar, Shear-zone systems and melts: feedback relations and self-organization in orogenic belts, *J. Struct. Geol.* 20 (1998) 211–227.
- [4] R.F. Weinberg, Mesoscale pervasive melt migration alternative to dyking, *Lithos* 46 (1999) 393–410.
- [5] E.W. Sawyer, C. Dombrowski, W.J. Collins, Movement of melt during synchronous regional deformation and granulite-facies anatexis, an example from the Wuluma Hills, central Australia, in: A. Castro, C. Fernandez, J.L. Vigneresse (Eds.), *Understanding Granites: Integrating New and Classical Techniques*, Geol. Soc. Lond. Spec. Publ. 168 (1999) 221–237.
- [6] A. Simakin, C. Talbot, Tectonic pumping of pervasive granitic melts, *Tectonophysics* 332 (2001) 387–402.
- [7] R.F. Weinberg, M.P. Searle, The Pangong Injection Complex, Indian Karakoram: a case of pervasive granite flow through hot viscous crust, *J. Geol. Soc. Lond.* 155 (1998) 883–891.
- [8] R.F. Weinberg, M.P. Searle, Volatile-assisted intrusion and autometasomatism of leucogranites in the Khumbu Himalaya, Nepal, *J. Geol.* 107 (1999) 27–48.
- [9] C.F. Miller, M.E. Watson, T.M. Harrison, Perspective on the source, segregation and transport of granitoid magmas, *Trans. R. Soc. Edinb.* 79 (1988) 135–156.
- [10] D. Vielzeuf, J.R. Holloway, Experimental determination of the fluid-absent melting relations in the pelitic system: consequence for crustal differentiation, *Contrib. Mineral. Petrol.* 98 (1988) 257–276.
- [11] J.B. Brady, The role of volatiles in the thermal history of metamorphic terranes, *J. Petrol.* 29 (1988) 1187–1213.
- [12] A.M. Leitch, G.F. Davies, M. Wells, A plume head melting under a rifting margin, *Earth Planet. Sci. Lett.* 161 (1998) 161–177.
- [13] O. Vanderhaeghe, C. Teyssier, R. Wisoczansky, Structural and geochronologic constraints on the role of melt from migmatites to leucogranites, during the formation of the Shuswap metamorphic core complex, *Can. J. Earth Sci.* 36 (1999) 917–943.
- [14] O. Vanderhaeghe, Pervasive melt migration from migmatites to leucogranite in the Shuswap metamorphic core complex, Canada: control of regional deformation, *Tectonophysics* 312 (1999) 35–55.